A Validated Model of a Complex Dust Collection System Using Mathcad

David L. Jones, Texas A & M University
B. K. Hodge, Mississippi State University

ABSTRACT

A generalized model of a complex dust collection system using Mathcad as the arithmetic engine is developed, the formulation technique is examined, the results are discussed, and the model is validated. The model results in a system of non-linear algebraic equations; one equation for each node in the duct system and one equation for each line segment in the duct system. Approaches to defining the major and minor losses are presented, and the structure of the Mathcad formulation is discussed. The model is validated by comparing the model results with experimental measurements from the modeled system. The uncertainties in the experimental measurements are assessed. The computed flow rates results agree within the experimental uncertainties for the most measured flow rates. The Mathcad-based model is accurate, easily implemented, and possesses significant potential for dust collector simulations.

Introduction

The removal of small airborne particles is an essential part of many industrial processes. Pneumatic conveying systems (dust collection systems) allow economical and reliable means of moving large quantities of airborne particles from the workplace to disposal locations. Dust collection systems are used in a wide variety of industries. The Environmental Protection Agency (EPA) and the Occupational Safety and Health Administration (OSHA) set standards for dust collection systems. The standards establish guidelines for the proper use of dust collection systems to ensure product quality and worker safety.

Energy consumption can be minimized if dust collection systems operate as efficiently as possible to properly remove dust particles. Oversizing and improper operation of dust collection systems can unnecessarily increase manufacturing costs by increasing energy costs. The current sizing methods for dust collection systems are set forth by the American Conference of Governmental Industrial Hygienists (ACGIH) in *Industrial Ventilation: A Manual of Recommended Practice* (ACGIH 1995).

Several factors must be taken into account for proper construction and operation of a dust collection system. A dust collection system operates by creating a pressure differential between two locations along a duct. The pressure differential causes airflow in the direction of the lower-pressure location. Air velocity within the system must meet or exceed the minimum transport velocity to keep the dust particles entrained. The recommended minimum transport velocity is the air speed at which the dust particles are fully suspended and traveling with the air stream. Dust particle size and weight are significant factors in determining the minimum transport velocity. The ACGIH manual (1995) presents minimum design velocities for the transport of various particulates. For example, the minimum recommended duct air velocity for sawdust is 4500 ft/minute. The recommended minimum

design velocities are higher than the theoretical and experimental values to account for factors such as plugging, damage to the ducts, leakage of ducts, and corrosion or erosion of the fan wheel.

A duct collection system is a series of ducts that have entrances at locations where dust control is necessary. Entrances to the dust collection system can be attached to machinery that produces dust in the process or in a general area where dust accumulates. A dust collection filter is a device that separates the air from the dust particles. Filter size and configuration are dependent on the amount of dust and the type of dust transported. A dust storage system is necessary to store accumulated dust until disposal.

Duct system design techniques and analysis procedures are presented in the ACGIH manual (1995), in the *ASHRAE Handbook, Fundamentals* (ASHRAE 1997), and in textbooks (such as McQuiston, Parker, & Spitler 2000). Many of these procedures are "approximate" in nature in the sense that complete system design calculations are time consuming and usually require numerical techniques that are not generally used by design firms. The approximate techniques permit relatively accurate design calculations to be made. Another concern of equal importance is the detailed analysis of an installed dust collection system. If a detailed analysis of an installed dust collection system were possible, then many what-if questions related to system operation could be answered. Extensive analyzes are generally not done by either consultants or owners since the time required to properly generate an analysis using traditional techniques can be prohibitive. However, with the use of recent arithmetic systems, such as Mathcad, systematic duct system models have become more feasible. This paper explores the generation, validation, and results of a Mathcad model for a relatively complex dust collection system. The procedure used is applicable to virtually any dust collection system.

System Description

The sawdust collection system considered was installed in 1990. The system is constructed of seven hundred and fifty-three feet of galvanized aluminum round sheet-metal ductwork and seventy-seven feet of flexible-plastic ductwork. The dust collection system is composed of 76 duct segments, 66 elbows, 33 wyes, 5 expansions, and 36 entrances plus a filter and a fan. Workstation dust control is achieved by five runs (legs) of aluminum and flexible-plastic ductwork ranging in size from 17 inches to 4 inches. The system is driven by a 31-inch centrifugal fan powered by a 100-hp motor. A filter separates the sawdust and the transport air. The filtered air can either be ducted back into the facility or exhausted to the outside. Figure 1 illustrates a schematic of the sawdust collection system.

Since a node is defined when two (or more) duct segments are joined to form a single segment, each duct segment is uniquely determined when the nodes specifying the two ends of a segment are specified. A model of the dust collection system is constructed by mathematically defining the system using the continuity equation at a node and the energy equation for steady-state, incompressible flow for a duct segment. A system of simultaneous equations is created using these two fundamental concepts. Mathcad software is used to solve the system of nonlinear simultaneous equations by finding the individual pressures at nodes and the individual section flow rates.

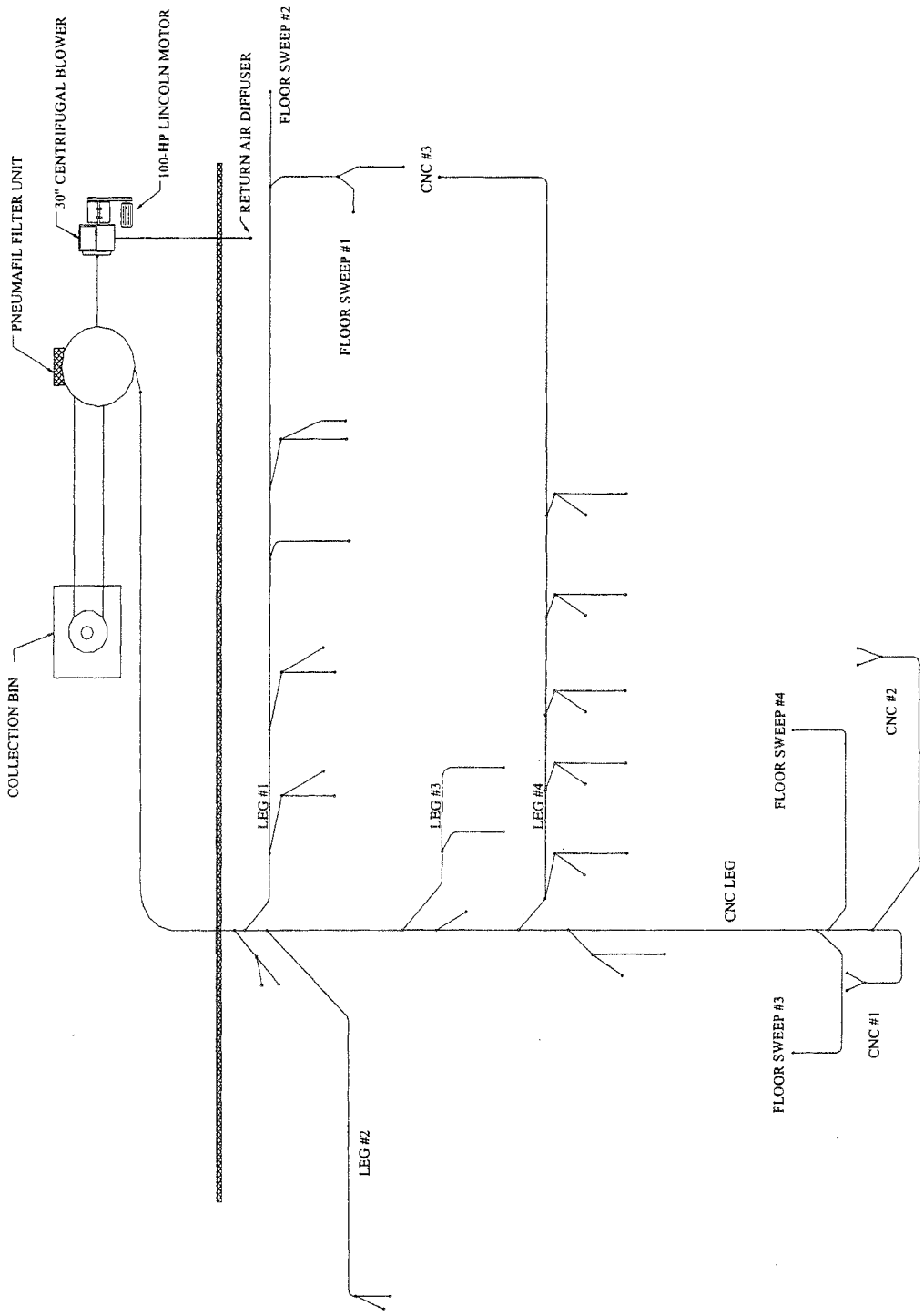

Figure 1. Dust Collection System Schematic

The continuity equation is applied at the intersection of wye connections where two or more flows combine or at junctions where diameters change. The mass flow rate of the air and sawdust entering a junction or connection must be equal to the mass flow rate leaving the junction or connection; that is

$$Q_1 = Q_2 + Q_3 \tag{1}$$

The energy equation for steady-state, incompressible flow will be used to determine the pressure differences within the system along a duct segment. Figure 2 illustrates a duct segment between nodes 1 and 2.

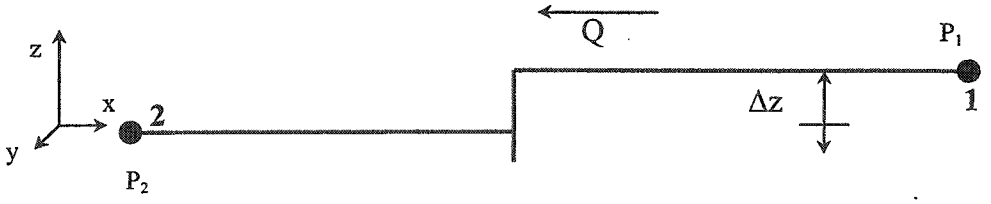

Figure 2. Schematic of a Duct Segment

The energy equation for the segment in Figure 2 is

$$P_1 + \frac{\rho V_1^2}{2} + \rho g z_1 = P_2 + \frac{\rho V_2^2}{2} + \rho g z_2 + \rho h_f + \rho h_c - \rho w_s \tag{2}$$

For a constant-diameter section with the flow of a low-density gas and no work addition, this equation can be reduced to

$$P_2 = P_1 - \rho h_f - \rho h_c \tag{3}$$

The head losses due to frictional forces (ρh_f) with the duct wall are termed major losses, and the head losses due to duct fittings (ρh_c) are termed minor losses. Using the Darcy-Wiesbach friction factor, the major losses can be expressed as

$$h_f = f \frac{L}{D} \frac{V^2}{2g} \tag{4}$$

A correlation provided by Haaland (1983) expresses the friction factor for turbulent flow as

$$f = \frac{0.3086}{\log\left[\frac{6.9}{\mathrm{Re}} + \left(\frac{\varepsilon}{3.7D}\right)^{1.11}\right]^2} \tag{5}$$

The dust collection system transports a combination of air and sawdust. The friction factor for a gas-solid flow differs from the friction factor of air and must be modified to take into account additional frictional forces caused by the entrained solid. Martin and Michaelides (1984) discuss five of the most widely utilized correlations to determine the friction factor of a gas-solid mixture for a horizontal, steady flow. They present a correlation for the total friction factor friction factor of a gas-solid flow (f_t) as a function of the mass flow rate of the solid transported, the mass flow rate of the gas transported, and the friction factor of the gas only (f_a). The total friction factor is calculated as a function of the ratio of the mass flow rate of the solid transported (M_{solild}) and the mass flow rate of the gas transported (M_{air}) and is given by Equation 6.

$$f_t = f_a \left(1 + \frac{M_{solid}}{M_{air}}\right)^{0.3} \tag{6}$$

The minor losses associated with flow through valves and fittings are expressed as

$$h_c = C\frac{V^2}{2g} \tag{7}$$

where C is the loss coefficient for the particular valve or fitting. Within the duct system, four types of fittings are encountered: elbows, wye connections, expansions, and entrances. The loss coefficient values, tabulated for general fittings, from Blevins (1984) were used in the dust collection model.

The sawdust is removed from the air stream by a filter that is between the dust collection system and the centrifugal fan. The filter, approximately nine feet in diameter and thirty-seven feet tall, resembles a cylinder standing on its end and filters the air stream by pulling the air and sawdust upward through a series of bags. The bags allow only the air to pass through, leaving the sawdust attached to the bags in the filter. The bags are cleaned by compressed air from nozzles that periodically blow air downward, forcing the sawdust to collect in the bottom of the filter. The sawdust is then fed into a second pneumatic conveying system and transported to a cyclone. The cyclone separates the sawdust from the air stream. The sawdust is gravity fed into a storage bin for offsite disposal.

The filter represents a significant pressure loss relative to the pressure loss of the entire dust collection system. Detailed operational data of such devices are seldom found within the industrial ventilation literature. The manufacturer was contacted and asked to provide information about the pressure loss across the filter in normal operational conditions. The company explained that the filter was originally specified for a maximum operational flow rate of 32,000 cubic feet per minute and a pressure drop through the filter of two to four inches of water. A more accurate pressure loss was found by measuring the static pressure upstream and downstream of the filter. The pressure drop across the filter was measured as 2.482 inches of water, which is within the range of the pressure loss through the filter suggested by the manufacturer. The static and stagnation pressures measured upstream of the filter were -13.5 and -11.7 inches of water, respectively. These values correspond to a duct velocity of 5,461 feet per minute and a flow rate of 28,624 cubic feet per minute.

The dust collection system is created from circular sections of aluminum ductwork. Elbows for the system are formed from several short circular aluminum sections cut at angles and assembled to form the radius of curvature desired. Blevins (1984) outlines a method to determine the loss coefficient for an elbow as a function of the ratio of the radius of the bend (R), the duct diameter (D), and the angle (θ) through which the elbow turns the flow and tabulates the loss coefficients for 20°, 30°, 45°, 75°, 90°, and 180° elbows

The dust collection system draws the air and sawdust mixture from an ambient space into the ductwork. Blevins states that the loss coefficient at an entrance flush with the wall at a right angle is 0.5. All base loss coefficients for entrances within the dust collection system model were taken as 0.5. Many entrances in the dust collection system are more complex than a flush inlet; these entrances require larger loss coefficients than the base loss coefficients and need special considerations. The entrance loss coefficients needing special considerations were experimentally determined. There are eleven duct sections where the loss coefficients were experimentally found. All special entrance loss coefficients were found in the same fashion used to find the filter pressure loss. The static and stagnation pressures within a duct were measured downstream of the entrance. The air velocity within the duct was calculated by applying Bernoulli's equation. The duct diameter and the calculated velocity were used to find the duct flow rate. The difference between the ambient

pressure and the static pressure downstream of the entrance was used within the energy equation to find the loss coefficient. Atmospheric pressure was always used as the ambient pressure outside of the entrance.

The dust collection system has four special 6-inch duct extensions called floor sweeps. These floor sweeps are labeled on the schematic (Figure 1) of the dust collection system. The floor sweeps extend from a main overhead line to the ground level. The floor sweeps open to ambient air with a five-inch by four-inch rectangular opening. Sawdust that has fallen to the floor is easily removed from the workplace by simply pushing the dust into the floor sweep. All four floor sweeps have a hinged door that is used to shut off the flow when the floor sweep is not in use. Since the literature does not cover the special case of floor sweeps, the loss coefficients were experimentally determined for both opened and closed floor sweeps.

The dust collection system is subdivided into five legs. Leg one has three radial arm saws, a ripsaw, and a whirlwind saw. Leg two has one rip saw. Leg three has two chop saws. Leg four has six band saws. CNC saws #1 and #2 are identical machines and are located on the CNC leg of the dust collection system. These saw locations are labeled on the schematic of the dust collection system. Several of the dust collection system entrances are directly attached to wood-cutting equipment. Special entrance effects for some direct connection are not covered in the literature, and the loss coefficients were experimentally determined.

Pressure taps were drilled into the duct connected to each type of saw to determine the entrance loss coefficient for that particular entrance. Loss coefficients were experimentally found for rip saw #1, chop saw #1, the whirlwind saw, CNC saw #2, and CNC saw #3. These entrance loss coefficients were then applied to the entrances of similar saws. The header system of CNC saw #2 is identical to that of CNC saw #1. Therefore, the experimentally-determined loss coefficient for the duct section leading to CNC saw #2 is applied to the duct section leading to CNC saw #1.

The dust collection system contains circular aluminum duct segments that become larger in diameter as the flow approaches the dust collection centrifugal fan. At a junction where the duct diameters change, an expansion fitting allows a smooth transition from one duct diameter to the next. Blevins (1984) expresses the pressure loss associated with an expansion fitting is a function of the diameters upstream (D_1) and downstream (D_2) of the fitting and the length (L) over which the expansion occurs.

The majority of the diameter changes within the duct collection system occur at expanding wye connections. The dust collections system contains main trunk lines and several branch ducts that intersect at these wye connections. Branch ducts and the main trunk lines may have differing stream velocities at the intersections. Flows from these two passages merge, and mixing of the streams occurs. Due to this mixing, an exchange of momentum takes place which results in an overall non-recoverable pressure loss. Losses associated with the convergence of the trunk line and the branch duct streams were calculated with the methods of Blevins. The losses associated with the convergence of two flows are a function of the angle of convergence of the two flows and the ratio of the two air velocities. The majority of the wye connections are expanding-wye fittings. These wye connections have a larger diameter trunk line after the branch duct. The larger trunk diameter duct accommodates the additional flow from the branch duct. Figure 3 illustrates a typical wye connection in the dust collection system. Blevins separates the loss coefficients for the wyes

into two components: a branch loss coefficient and a main trunk line loss coefficient. The loss associated with the flow from the branch line entering into the main trunk line is the branch loss component. This loss is attached to the branch duct section loss coefficient. The loss associated with the flow of the main trunk line prior to and after the addition of the branch flow is the main trunk line loss component. This loss is attached to the main trunk duct section loss coefficient prior to the wye connection. Blevins presents loss coefficients for convergence angles (θ) of 60°, 45°, and 30°. All thirty-three wyes within the dust collection model have an angle of convergence of 60°.

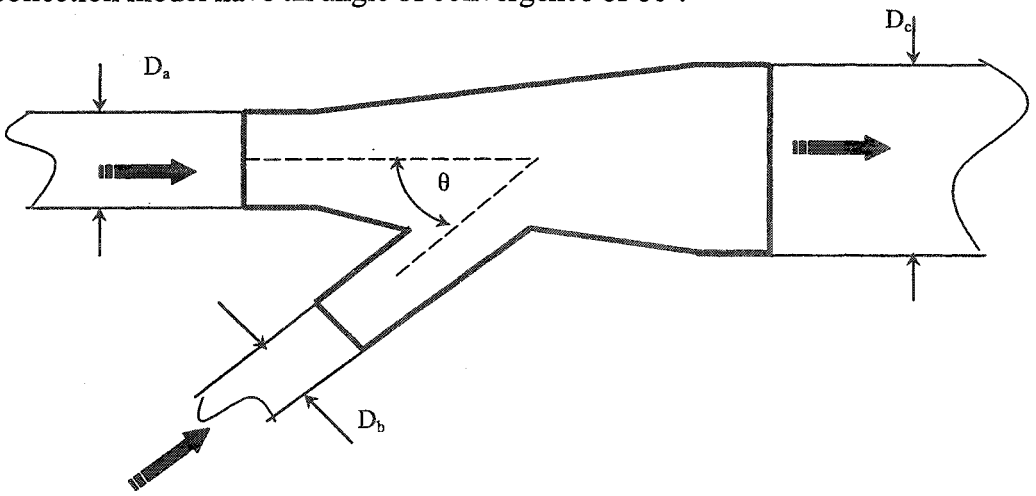

Figure 3. Schematic of a Wye onnection

The loss coefficient of a wye fitting is a function of the fluid velocities through the sections. However, the fluid velocities are not initially known. The dust collection system model must be manually iterated with guessed loss coefficients for the wye fittings as starting points. The fluid velocities from the model with guessed loss coefficients are then used to find a better estimate for the wye loss coefficients. This process is repeated until the loss coefficients do not change. The process converges rapidly and only a few iterations are required.

Mathcad Solution

The professional version of Mathcad 2000 software from MathSoft Inc. was used to solve the system of simultaneous equations that models the dust collection system. The solution is unique to the initial pressure at node one (the fan inlet) of the dust collection model. This pressure was measured as 13.5 inches of water below atmospheric. If this initial pressure were to change, the system solution would also change.

Forty conservation of mass equations and seventy-six energy equations are required to model the dust collection system. The resulting system contains 116 total equations (with 116 unknowns).

Due to the size of the system of simultaneous equations and the underlying equations within the system, changes to the calculation defaults settings (TOL and CTOL for readers familiar with Mathcad) were necessary to ensure a solution. To verify that the changes to the calculation settings did not affect the validity of the solution, the solution was checked by

confirming that the pressures and flow rates calculated satisfied each individual equation. Checking the solution of the dust collection model confirmed that the model works properly and that the changes in the default settings did not degrade the accuracy of the solution.

The Mathcad worksheet for the simulation of the dust collection system is 40 pages long. However, it is very easy to assemble and can be used to model other dust collection systems by just adding/deleting/changing the input values. The length of the worksheet precludes a complete listing in this paper. The worksheet can be conveniently divided into eight segments, (1) definitions of constants, (2) definition of duct segment lengths and diameters, (3) specification of function definition equations (such as the Haaland equation for the friction factor), (4) specification of known pressures (inlets and fan suction side), (5) guessed values of intermediate pressures and duct segment flow rates and specification of the loss coefficients, (6) Mathcad Given/Find block defining the system of non-linear algebraic equations, (7) the solution output (flow rates and intermediate pressures), and (8) interpretation of the solution.

Validation

Twenty-five static and stagnation pressure measurements were taken to validate the solution of the mathematical model. Nine pressure measurement locations are on a main trunk line. The remaining sixteen pressure measurement locations are on duct sections that contain an entrance.

Holes were not drilled directly into wye connections or expansion fittings. Therefore, pressure measurement locations do not coincide with the locations of calculated intermediate pressures. This was purposely done in order to avoid regions of mixing and expanding flow found in wye fittings and expansion fittings. The twenty-five pressure-measurement taps were located in straight duct sections and as far from fittings as possible.

Duct diameters of the dust collection system range between 31-inches and 4-inches. Two different size pitot probes were used to obtain pressure measurements. Probe one is seven and one-half inches in length and one-eighth inch in diameter. Probe one was used to obtain pressure readings within ducts nine inches to four inches in diameter. Probe two is sixteen inches in length and three-sixteenths inch in diameter. Probe two was used to obtain pressure readings within ducts thirty-one inches to fifteen inches in diameter.

There are two methods for estimating mass flow rates, a single pressure measurement at the duct centerline and an equal-area pressure measurement method. Pressure measurements at the duct centerline ensure that the measurements are maximum velocity measurements. Previous research conducted by Schmidt (1999) concluded that for this system the difference between the results of the two methods was less than two percent. Schmidt measured the flow rate through a thirty-one inch diameter duct. The single pressure method yielded an air velocity of 8,600 feet per minute and the equal area method yielded an air velocity of 8,763 feet per minute. Therefore, the centerline method for taking air velocity measurements was used.

Twenty-five static and stagnation pressure measurements were taken while the dust collection system was in a normal mode of operation. Although the mathematical model of the dust collection system is a steady-state representation, the actual pressure measurements had a small oscillatory action within the system. This oscillatory action was more prevalent in the larger ducts and especially in the main trunk line. A slow, steady oscillation around a

mean value was observed when measuring pressures within larger ducts close to the dust collection filter. The static pressure measured at node one directly upstream of the centrifugal fan oscillated between -12.5 and -14.5 inches of water. The mean static pressure was observed as –13.5 ± 1-inch water. The dust collection filter is constantly cleaned by periodically injecting a blast of compressed air into the dust collection bags. This self-cleaning action accounts for some of the pressure fluctuations measured.

The twenty-five static and stagnation pressure measurements were used to calculate the air velocities within the duct sections by applying Bernoulli's equation. These velocity calculations along with the respective section diameters were then used to calculate section flow rates. The total flow rate through the dust collection system was measured as 28,624 cubic feet per minute.

The uncertainties associated with the flow rates were estimated using the procedures of Coleman and Steele (1999). The bias uncertainties associated with the pressure measurements are a function of the accuracy of the gauge. Accuracy of the pressure gauges is taken from the manufacturer's data as 2% of the full-scale value. Precision uncertainty of the pressure measurements is a function of the unsteadiness of the pressure measurements. Unsteadiness of the pressure measurements was observed as three and one-half percent of the readings. Static and stagnation pressure readings were taken. Each reading has its own individual precision uncertainty. The total uncertainty associated with the pressure measurements (U_{Press}) is calculated using

$$U_{Press} = \left(UB^2 + UP^2\right)^{0.5} \tag{8}$$

where UB is the bias uncertainty of the instrument and UP is the precision uncertainty of the measurement due to the unsteadiness of the pressure reading. The total uncertainty for each static and stagnation pressure measurement was calculated using Equation (8). Forty-eight of the fifty pressure measurements have a percent uncertainty less than ten percent of the readings. The two reading that have a percent uncertainty greater than ten percent were measured at locations of very low flow rates.

The uncertainty of a flow rate measurement has five elemental uncertainties: the static pressure, the stagnation pressure, the fluid density, the duct diameter, and the correlated bias uncertainties of the pressure measurements. The same pressure gauge was used to take the static and stagnation pressure readings for each individual measurement. Therefore, the bias uncertainties of the pressure measurements are correlated. Since the difference between the static and stagnation pressures is used to find the volumetric flow rate, the correlation between these two measurements will decrease the total volumetric flow rate uncertainty.

The bias uncertainty of the fluid density (U_ρ) is five percent of the value or 3.625×10^{-3} lb/ft^3. The bias uncertainty of the duct diameters (U_D) is three percent of the diameter. The uncertainty in the flow rate is computed as the root-sum-square of the products of the sensitivity coefficients with each of the elemental uncertainties and is expressed as

$$U = \left[\left(\frac{dQ}{dP_{stagnation}} U_{stagnation} \right)^2 + \left(\frac{dQ}{dP_{statien}} U_{static} \right)^2 + \left(\frac{dQ}{d\rho} U_\rho \right)^2 + \left(\frac{dQ}{dD} U_D \right)^2 + \left(2 \frac{dQ}{dP_{stagnation}} \frac{dQ}{dP_{static}} UB^2 \right)^2 \right]^{0.5} \tag{9}$$

where the derivative terms are the sensitivity coefficients, the U terms are the uncertainties, and UB is the bias uncertainty.

The strategy to validate the Mathcad dust collection model is to compare the measured volumetric flow rates to the calculated volumetric flow rates. Table 1 presents the measured volumetric flow rates and their uncertainties and the calculated volumetric flow rates for the duct sections measured. Twenty-one of the twenty-five volumetric flow rates from the Mathcad model fall within the uncertainty bands of the volumetric flow rate measurements. The volumetric flow rates that do not fall within the measurement uncertainty bands are at measurement locations X6, X7, X16, and X21. The larger modeled volumetric flow rates fall within the uncertainty band of the measured volumetric flow rates.

Table 1. Measured Volumetric Flow Rates and Uncertainties and Calculated Volumetric Flow Rates

Pressure Measurement Node	Duct Section Number	Measured Flow Rate (ft^3/min)	Uncertainty of the Measured Flow Rate (ft^3/min)	Modeled Flow Rate (ft^3/min)	Calculated Within Uncertainty Limits
1	1	28,624	5,308	25,516	yes
X1	2	28,624	3,982	25,516	yes
X2	7	6,702	900	5,937	yes
X3	13	911	66	995	yes
X4	14	715	65	694	yes
X5	18	112	266	99	yes
X6	22	79	10	66	no
X7	23	876	156	1,120	no
X8	25	357	280	196	yes
X9	26	619	151	677	yes
X10	27	357	324	248	yes
X11	32	19,981	4,218	16,259	yes
X12	30	876	136	801	yes
X13	35	355	63	339	yes
X14	36	389	62	340	yes
X15	44	7,625	970	7,133	yes
X16	46	562	46	502	no
X17	47	1,072	107	1,203	yes
X18	58	502	43	477	yes
X19	60	486	525	478	yes
X20	61	505	191	478	yes
X21	67	1,072	112	940	no
X22	69	253	523	254	yes
X23	70	2,128	336	2,150	yes
X24	74	758	155	726	yes

Considering the complexity of the dust collection system, the difficulties in obtaining pressure measurements in an operating manufacturing facility, and the general nature of the minor loss coefficients for the system, the model performance is good. Certainly the level of

agreement between the measured and calculated flow rates is adequate to answer any questions relating to system modification and performance.

Solution Summary

The driving force in the dust collection system is the pressure differential induced by the centrifugal fan. The total power lost through the entire system is equal to the power input by the centrifugal fan. The total power input was calculated as 44.73 kW. Power loss is subdivided into four categories in order to determine the major factors that dictate energy loss in the system. The four categories are as follows: (1) the power lost through the dust collection filter, (2) the power lost due to duct wall friction, (3) the power lost due to flexible-duct wall friction, and (4) the power lost due to duct fittings.

Table 2. System Power Losses

Power Losses	Symbol	Total Power Lost (Watts)	Percent of Total Power Lost (%)
Dust Collection Filter	E_{filter}	7,420	18.3
Aluminum Duct Work	EL_N	7,049	17.5
Flexible Duct Work	EL_{N_flex}	811	2
Duct Fittings	EC_N	25,081	62.2
Total	———	40,361	100

Table 2 shows that the power loss within the dust collection system is dominated by the losses due to flow through duct fittings. The power losses due to both aluminum and flexible-duct wall friction combine for approximately twenty percent of the total.

Conclusions

Twenty-one of the twenty-five modeled volumetric flow rates agree within the uncertainty bands of the measured volumetric flow rates. The modeled volumetric flow rates along the main trunk line all fall within the uncertainty bands of the measured volumetric flow rates. More importantly, the total modeled volumetric flow rates through the entire dust collection system is within the uncertainty band of the total measured volumetric flow rate through the system. The total measured volumetric flow rate of the dust collection system is 28,624 cubic feet per minute with an uncertainty of 5,308 cubic feet per minute. The total modeled volumetric flow rate of the dust collection system is 25,516 cubic feet per minute. The dust collection system transports a combination of air and sawdust. The model compensates for the additional frictional forces caused by the entrained sawdust in the airflow by utilizing a correlation for a gas/solid flow from Martin and Michaelides (1984). Since the mass of the sawdust transported is much less than the mass of the air transported, the additional frictional force due to the entrained sawdust is negligible. The use of the Blevins (1984) loss coefficients provided a method to account for the pressure losses due to duct fittings (minor losses) within the dust collection system. Although there exists more complex techniques to determine pressure losses of fittings than the general values presented

in Blevins, his coefficients proved sufficient to model the wide variety of minor losses within the dust collection system. The model showed that the dust collection system power losses are dominated by minor losses. Duct fittings accounted for over sixty-two percent of the total power loss of the system.

The Mathcad approach to modeling a dust collection system has been validated. This approach offers a simple, generalized procedure that is easily implemented. Using the Mathcad approach, what if questions about the system can easily be answered.

References

American Conference of Governmental and Industrial Hygienists (ACGIH). 1995. *Industrial Ventilation: A Manual of Recommended Practice.* 22nd ed. United States: ACGIH, 1995.

ASHRAE. 1997. *ASHRAE Handbook, Fundamentals.* Atlanta: ASHRAE.

McQuiston, F. C., Parker, J. D., and Spitler, J. D. 2000. *Heating, Ventilating, and Air Conditioning Analysis and Design.* 5th ed., New York: Wiley.

Haaland, S. E., 1983. "Simple and Explicit Formulas for the Friction Factor in Turbulent Flow," *Trans. ASME J. Fluids Engineering* 105(3):89-90.

Martin, J., and Michaelides, E. 1984. "A Critical Review of Frictional Pressure-Drop Correlations for Gas-Solid Flows." In *Multi-Phase Flow and Heat Transfer III: Proceedings of the Third Multi-Phase Flow and Heat Transfer Symposium Workshop.* Netherlands: Elsevier.

Blevins, Robert D. 1984. *Applied Fluid Dynamics Handbook.* New York: Van Nostrand Reinhold.

Schmidt, David F. 1999. "Validated Model of a Dust Collection System", MS Thesis, Mississippi State, MS: Mechanical Engineering Department, Mississippi State University.

Coleman, H. W., and Steele, W. G. 1999. *Experimentation and Uncertainty Analysis for Engineers.* 2nd ed. New York: Wiley.